

Effect of growth rate on the size, composition, and optical properties of InAs/GaAs quantum dots grown by molecular-beam epitaxy

P. B. Joyce, T. J. Krzyzewski, G. R. Bell, and T. S. Jones*

Centre for Electronic Materials and Devices, Department of Chemistry, Imperial College, London, SW7 2AY, United Kingdom

S. Malik, D. Childs, and R. Murray

Centre for Electronic Materials and Devices, Department of Physics, Imperial College, London SW 2BZ, United Kingdom

(Received 26 April 2000; revised manuscript received 28 July 2000)

The effect of the InAs deposition rate on the properties of InAs/GaAs quantum dots (QD's) grown on GaAs(001) substrates by molecular-beam epitaxy has been studied by scanning tunneling microscopy (STM) and photoluminescence (PL). PL studies performed on GaAs capped QD samples show that the emission wavelength increases with decreasing growth rate, reaching a maximum around $1.3 \mu\text{m}$, with the linewidth decreasing from 44 to 27 meV. STM studies on uncapped dots show that the number density, total QD volume, and size fluctuation all decrease significantly as the growth rate is reduced. We deduce that the composition of the dots is also dependent on the growth rate, the indium fraction being highest at the lowest growth rates. The shifts in the emission wavelength and linewidth correlate with changes in the QD size, size distribution, and composition.

I. INTRODUCTION

The growth of self-assembled InAs/GaAs quantum dots (QD's) has been studied extensively over the past few years since these structures offer the prospect of temperature-independent, ultralow-threshold lasers.¹ Despite considerable effort worldwide, however, there is still no consensus on key issues such as island size, shape, and composition.^{2,3} Nevertheless, many groups are exploring the possibilities of modifying these properties through changes in the growth conditions.⁴ Perhaps the most exciting prospect is the extension of the emission to longer wavelengths using submonolayer deposition,^{5,6} atomic layer epitaxy,⁷ punctuated growth,⁸ strain-reduced overgrowth,⁹ and low growth rates.¹⁰⁻¹³ This offers the possibility of producing devices that operate at $1.3 \mu\text{m}$ but are grown on GaAs substrates. These would have a clear advantage over InP-based structures, since the processing technology is more mature and quarter-wave layers of GaAs and AlAs can be used as distributed Bragg mirrors.^{12,14}

We have recently demonstrated that very low InAs growth rates lead to InAs/GaAs QD structures that exhibit room-temperature emission at $\sim 1.3 \mu\text{m}$.¹⁰ Preliminary atomic force microscopy (AFM) studies on the uncapped QD's suggested that the reduced growth rate leads to larger dots and a more uniform size distribution, the latter consistent with the improved optical linewidths.¹⁰ A more recent paper by Nakata *et al.*¹³ has confirmed these observations and their AFM results showed that the number density of the dots decreases significantly with decreasing InAs deposition rate.

In this paper, we present a more quantitative study of the effects of the InAs growth rate on the optical properties and composition of InAs/GaAs QD's grown on GaAs(001) substrates by molecular-beam epitaxy (MBE). Scanning tunneling microscopy (STM) and photoluminescence (PL) measurements carried out on uncapped and GaAs capped QD's

show that the growth rate has a strong influence on their size, composition, and optical properties. Reducing the growth rate results in a decrease in the QD number density and volume, an increase in the room-temperature emission wavelength to $1.3 \mu\text{m}$, and a systematic reduction in the emission linewidth. The volumes obtained from the STM measurements on uncapped samples indicate that the composition of the dots changes with growth rate, with the indium fraction being greatest at the lowest growth rate.

II. EXPERIMENT

The samples were grown in a combined MBE-STM growth system (DCA Instruments/Omicron GmbH) that is also equipped with reflection high-energy electron diffraction (RHEED) for *in situ* monitoring of growth and calibration of fluxes. Epi-ready GaAs(001) substrates (n^+ Si-doped) were mounted onto molybdenum plates and transferred directly into the growth chamber via a fast entry lock. After initial thermal cleaning at 300°C , the native oxide layer was removed under an As_2 flux at 620°C . A GaAs buffer layer was grown at 590°C and the substrate temperature was reduced to 490°C for the deposition of 200 \AA of GaAs. InAs was deposited at different rates in the range $0.55\text{--}0.0065 \text{ ML s}^{-1}$ and the 2D \rightarrow 3D growth mode transition was followed by monitoring the change in the RHEED pattern along the [110] direction. The In flux was calibrated by monitoring RHEED oscillations during homoepitaxial growth of InAs(001) at different In fluxes, and these data were extrapolated to give cell temperatures for the lowest growth rates. The background As_2 pressure was maintained at 4×10^{-6} Torr during growth of all the samples.

After InAs deposition, some of the samples were transferred immediately to the STM chamber (within a few seconds) and allowed to cool to room temperature (several minutes).¹⁵ This quenching process is much more rapid than achieved in conventional MBE growth chambers and allows

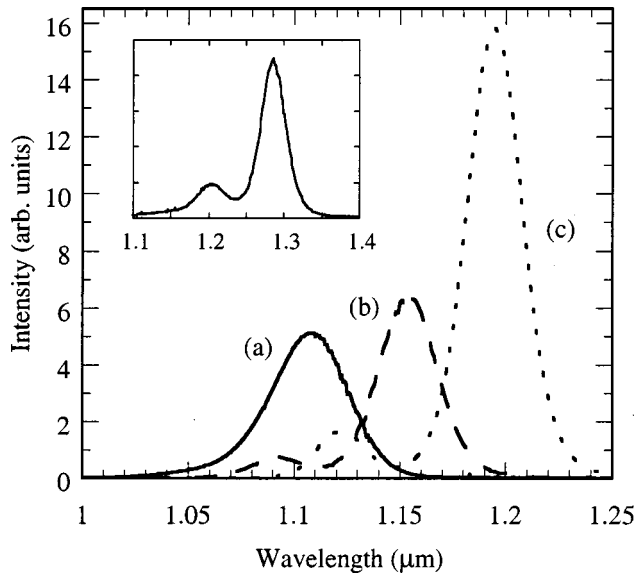


FIG. 1. Low-temperature (10 K) PL emission spectra obtained from GaAs capped InAs/GaAs QD samples grown on GaAs (001) substrates at (a) 0.55, (b) 0.016, and (c) 0.0065 ML s^{-1} . In all cases 2.7 ML of InAs was deposited at 490 °C. The inset shows the emission from sample (c) at 300 K.

us to “freeze” the QD’s for detailed STM imaging, avoiding the problems associated with continued growth through alloying and segregation during longer cool-down periods. Constant-current STM images were obtained with a sample bias of -3.5 V and tunneling currents of 0.05–0.2 nA. Some of the uncapped samples were also removed for *ex situ* AFM analysis. A second series of samples were grown for PL measurements. The structure was identical to those described above, but the islands were immediately overgrown with 200 Å of GaAs at 490 °C and the temperature was then increased to 590 °C for deposition of a further 500 Å of GaAs. PL measurements were carried out at 10 and 300 K. A HeNe or Ar⁺ laser was used to create electron-hole pairs; the luminescence was dispersed with a SPEX 1404 monochromator and detected with a cooled Ge photodiode and lock-in amplifier.

III. RESULTS AND DISCUSSION

Low-temperature PL spectra from capped QD samples grown at different rates are shown in Fig. 1. The emission wavelength increases to 1.2 μm for the QD sample grown at 0.0065 ML s^{-1} (c). There is a concomitant narrowing of the linewidth from 44 to 27 meV consistent with a narrower size distribution. The inset shows the room-temperature emission for the QD sample grown at 0.0065 ML s^{-1} . At 300 K there is no increase in the linewidth and the intensity is reduced by a factor of only 8. It should be noted that these samples are grown without any confining GaAs/AlAs superlattice surrounding the dot layer and the rather small reduction in intensity is a result of the deeper confining potential in the low growth rate QD’s. Although the redshift does correlate with the known increased size of the 3D islands,¹⁰ we believe that this alone cannot account for the measured shift and an additional explanation is required, namely that the low growth rate QD’s have a higher indium fraction. Nevertheless, the

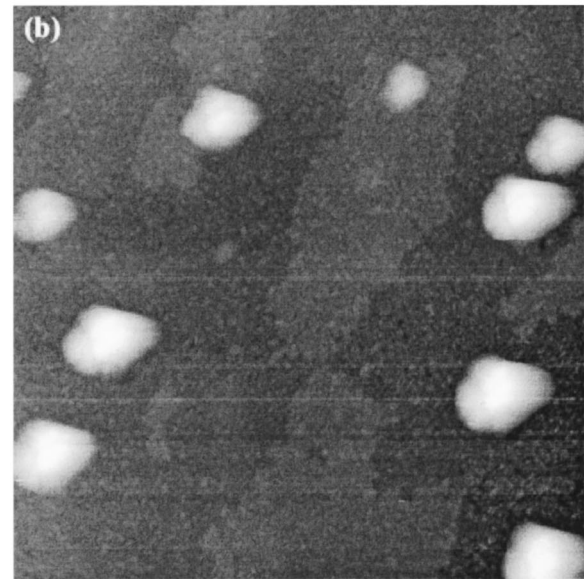
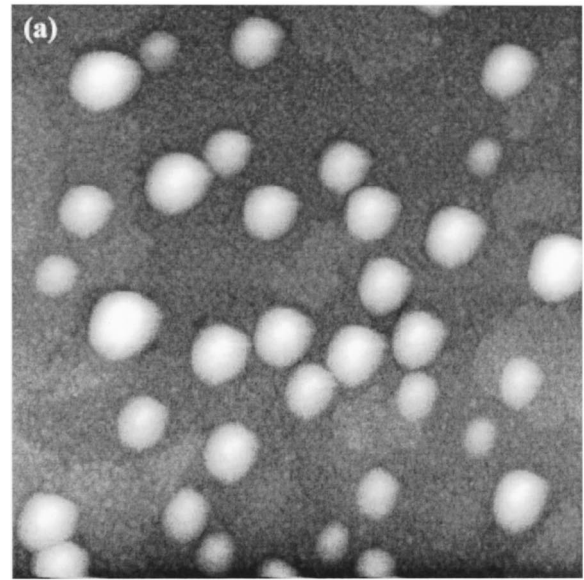


FIG. 2. STM images ($0.2 \times 0.2 \mu\text{m}^2$) of 2.2 ML of InAs deposited on GaAs(001) at 490 °C with rates of (a) 0.094 ML s^{-1} and (b) 0.016 ML s^{-1} .

increased emission intensity and reduced linewidth are both expected to be beneficial for the development of QD lasers.

The two STM images shown in Fig. 2 were taken after the deposition of 2.2 ML of InAs on GaAs(001) at 490 °C at growth rates of (a) 0.094 ML s^{-1} and (b) 0.016 ML s^{-1} . Statistical differences between the QD’s produced at the two rates are shown in Table I, derived from at least ten images (>100 QD’s). The QD number density (N_s) is reduced significantly at lower growth rates, while the island mean height (h) and mean diameter (d) become larger. The height fluctuation ($\Delta h/h$) of the QD’s is also reduced at the lower growth rates. The increase in size and decrease in size fluctuation for the lower growth rate samples provide a plausible explanation for the reduction in the inhomogeneous linewidth of the emission.

The average QD volume was determined by directly integrating STM images using standard image-processing software and no assumption was required about the actual shape

TABLE I. Statistical properties of QD's produced at two different growth rates, as measured from STM images of uncapped InAs-GaAs samples.

Growth rate (ML s ⁻¹)	Number density, N_s (10 ¹¹ cm ⁻²)	Height, h (Å)	Diameter, d (Å)	Height fluctuations, $\Delta h/h$
0.094	1.0	20	150	22%
0.016	0.2	35	200	16%

of the dots. Figure 3(a) is a plot of the total QD volume (converted into monolayer equivalents) as a function of growth rate for a fixed deposition of 2.2 ML of InAs. The major sources of error in the volume measurements are variations in growth temperature (± 10 °C) and deposition time (± 1 s), the latter due to manual operation of the In shutter. Tip convolution effects can also lead to increases in the apparent QD volume, although this was minimized by optimizing tip treatment procedures and rejecting data sets

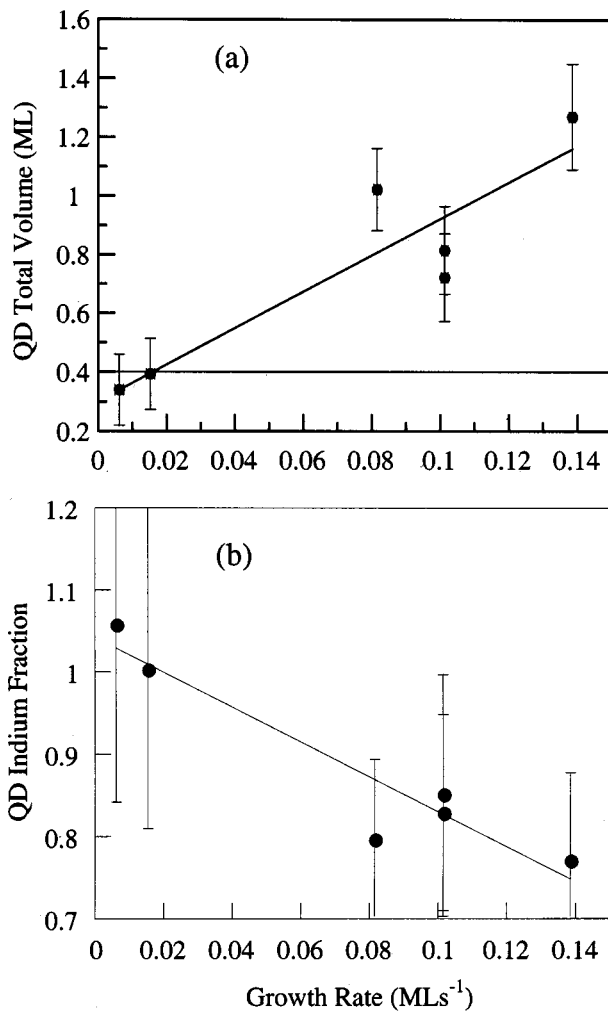


FIG. 3. (a) The total QD volume (monolayer equivalents) measured directly from STM images plotted as a function of InAs deposition rate. The solid horizontal line is the volume expected assuming classic Stranski-Krastanov growth. (b) The In fraction within the QD's as a function of growth rate. Each data point was calculated from the total QD volume measurements assuming that the wetting layer undergoes some erosion, but has a composition that is fixed at $\text{In}_{0.67}\text{Ga}_{0.33}\text{As}$.

where tip convolution is apparent. Tip convolution is generally easier to identify in STM than AFM due to the irregular nature of the etched tungsten tips. An example of an irregular tip shape is evident in Fig. 2(b) and is repeated for each QD in the image. This image was not used for statistical analysis.

It is clear from Fig. 3(a) that there is a gradual decrease in the total QD volume as the growth rate is reduced. The solid horizontal line represents the predicted total QD volume if growth occurred by a classic Stranski-Krastanov (SK) mechanism with a critical thickness of 1.8 ML. The two volumes are comparable at the lowest growth rates, but are significantly different at the higher rates, with the measured QD volume being greater by ~ 0.8 ML at a growth rate of 0.13 ML s^{-1} .

The volume measurements can be used to determine the composition of the 3D islands, although this requires knowledge of the total In content of the 2D wetting layer (WL) after QD formation.^{3,16} Our STM studies indicate the presence of a (1×3) surface reconstruction, a known characteristic of $\text{In}_x\text{Ga}_{1-x}\text{As}$ alloy formation in the 2D growth of InAs on GaAs(001).¹⁷⁻¹⁹ This suggests that a significant amount of InAs remains between the islands in the WL after QD formation, but this quantity is not necessarily equal to 1.8 ML.¹⁶ Figure 3(b) is a plot of the In fraction in the QD's, assuming that additional QD material arrives from erosion of the WL, which has a fixed composition of $\text{In}_{0.67}\text{Ga}_{0.33}\text{As}$.¹⁷⁻¹⁹ In a previous study, we determined the composition of the QD's at different growth temperatures by assuming that the In content of the WL was fixed and that erosion of the GaAs substrate occurred.³ In that case, the presence of Ga in the QD's could be unambiguously determined at the highest temperatures since the QD volumes were greater than the *total* amount of InAs deposited. The QD compositions shown in Fig. 3 are approximate because the In content of the WL after QD nucleation cannot be determined by STM alone. In fact, recent reflection anisotropy experiments have suggested that the WL thickness may actually increase even after QD nucleation.¹⁶ This would enhance the Ga content of the QD's compared to the figures given here.

The data in Fig. 3 imply that ideal SK growth occurs at the lowest rates and the QD's are pure InAs. As the growth rate is increased, however, In and Ga can both be incorporated from the WL into the QD's and the In fraction drops to a value of about 80% at 0.13 ML s^{-1} . The greater In content at the lowest growth rates together with the increased average size provides a good explanation for the observed redshift in emission wavelength. It should be noted that further changes in the composition and thickness of both the QD's and WL are known to occur after capping,² although the capping process is identical for all our samples. It is reason-

able to expect that a higher precapping In content would result in a higher In fraction in the capped QD's.

Recent reports have indicated improved emission properties using growth-interrupt techniques.⁸ We have investigated the combination of interrupted growth and low growth rates in a series of samples nominally identical to those described above. In all cases these samples are optically inferior; the linewidths are increased and the emission wavelengths are blueshifted relative to their continuous growth counterparts. Furthermore, changes in the V:III ratio made by altering the As flux also provide a means of altering the emission wavelength. However, increasing the As₄ pressure at fixed In flux (0.04 ML s⁻¹) has been shown to cause a blueshift in the emission.⁸ Our results show that simple changes in the In flux provide the most straightforward way of controlling the optical properties of InAs/GaAs QD's, in particular for long-wavelength applications.

IV. QD GROWTH MECHANISMS

We now discuss the QD growth mechanisms in light of the observed growth-rate-dependent changes, also recalling the temperature-dependent changes in QD composition outlined in Ref. 3. In particular, we compare the experimental results with some recent theoretical studies, one of which employs energetic calculations²⁰ and two which use mean-field rate equations to model the growth process.^{21,22} Of course, energetic calculations do not take into account the kinetics of growth, but instead give equilibrium characteristics. We would generally expect to approach this equilibrium limit more closely at lower growth rates. On the other hand, rate equations for growth are naturally sensitive to the effects of deposition rate. However, in order to construct such a growth model, the allowed surface processes must be chosen (e.g., attachment of adatoms to islands and the transformation of 2D to 3D islands) and rates for these processes must be deduced or calculated. In the case of InAs-GaAs QD formation, it is still not certain what the most important processes are. We propose that strain-enhanced detachment of both In and Ga atoms from the WL is a crucial process which influences the composition of the QD's and must be considered in any realistic growth model.

It is important to stress that our RHEED and STM experiments provide no evidence for any growth-rate dependence of the critical thickness and WL. There is independent evidence from grazing incidence x-ray-diffraction measurements for a "locked-in" surface composition of In_{0.67}Ga_{0.33}As for (In, Ga)As(001) surfaces.¹⁹ We therefore assume in the following discussion that the WL surface on which QD nucleation and growth occurs is essentially identical for all growth rates prior to the 2D-3D growth mode transition.

The STM results clearly demonstrate that the lower growth rates favor a smaller QD number density, although the starting surface is the same. Several models have been proposed for the 2D-3D transition that explicitly involve the transformation of 2D islands or "platelets" into 3D islands.²¹⁻²⁴ The model of Priester and Lannoo²³ involves platelets of lateral dimension ~ 600 Å and a minimum estimated QD size of ~ 16 000 atoms. The latter value is inconsistent with our STM measurements, in which we observe

3D features with sizes < 1000 atoms close to the critical coverage. We note that large 2D features are frequently observed; for example, in Fig. 2(b), two islands with heights of ~ 3.0 Å and lateral dimensions of 100–1000 Å can be seen. However, these should be interpreted as preexisting islands formed during the surface structure transition from GaAs(001)-(2 \times 4) to c(4 \times 4).²⁵ Since a QD is sited on top of each island in Fig. 2(b), it is clear that these features are not precursors to 3D islands.

The mean-field rate equation theory of Dobbs *et al.*²¹ is rather more generic in that it makes few assumptions about the nature of initial 2D islands, although it does presuppose their existence as the precursor to QD's. This model was used to reproduce the dependence of the 3D island density on growth rate and temperature in the metal-organic vapor phase epitaxial growth of InP- on GaP-stabilized GaAs(001).²¹ Higher island densities were found at low temperatures and high growth rates, in qualitative agreement with the present and previous³ results for InAs-GaAs(001) MBE growth. This model provides a framework for understanding the reduction in QD number density with reduced growth rate, even if the microscopic processes are not known in detail. Further experimental work close to the critical coverage should shed more light on the relevant atomistic pathways and enable more detailed models to be constructed.

Using quite general free-energy calculations, Tersoff²⁰ has shown that when a 3D island nucleates from a strained alloy WL, the composition of the island is enhanced in the misfitting component (In) over the composition of the WL. Applying Tersoff's analysis, the predicted equilibrium QD composition is around In_{0.9}Ga_{0.1}As for 3D island growth from an In_{0.67}Ga_{0.33}As WL at typical growth temperatures. As the temperature is lowered, the theory predicts an even higher In fraction because of the reduced energy contribution arising from the entropy of mixing (the entropy prevents the islands from ever achieving a pure InAs composition).²⁰ This qualitative temperature dependence is also found in our earlier experiments performed at a fixed growth rate of 0.3 ML s⁻¹,³ although the range of variation of composition with temperature is significantly larger than predicted by the equilibrium theory. This indicates the strong influence of the growth kinetics on the final QD composition, as pointed out by Tersoff.²⁰ The suggestion that the growth kinetics play a major role in determining the final composition is confirmed by the present measurements. In the absence of kinetic limitations, there would be no change with growth rate at fixed temperature. However, a mechanism by which growth-rate-dependent QD alloying occurs is required.

A more recent theoretical model for QD formation has explicitly included strain-enhanced *In adatom detachment from QD's*,²² generalizing the model of Dobbs *et al.*²¹ The strain fields causing this effect arise from the QD's themselves, and although their detailed form is not known, they are modeled in Ref. 22 as declining with the cube of distance from the QD and increasing proportionally with the QD volume. The lowering of the detachment barrier for group-III atoms is linear with this strain. Using the experimentally determined mean QD separation and volume for growth rates of 0.094 and 0.016 ML s⁻¹, the effects of these strain fields on adatom detachment barriers are significantly larger for the higher growth rate (with smaller but more densely packed

QD's). In fact, using the proportionality constant given in Ref. 22, the change of detachment barrier derived is very large (as high as 1 eV), although as the authors point out, this constant is difficult to calculate and their parametrization of the strain-field form is approximate. The barrier reduction is three times larger for the QD arrays produced at the growth rate of 0.094 ML s^{-1} than at 0.016 ML s^{-1} . The relative barrier reduction between the different growth rates should be even larger at the early stages of QD growth, where there is still a large difference in QD density but the sizes have not yet diverged.

We believe that these strain fields may lead principally to increased *In* and *Ga* adatom detachment from the WL rather than from QD's. The strain fields due to QD's are mediated by the WL, in which strain relief is likely to be inefficient compared with the majority of the surface of a QD. This would produce a higher strain environment in the WL close to a QD. Of course, the details of detachment probabilities also depend on the surface atomic structure on the QD surface²⁶ and the WL surface as well as on the local strain. However, strain-induced detachment of both In and Ga atoms from the WL can explain the growth-rate-dependent alloying of the QD's, at least qualitatively. Dobbs *et al.*²¹ mentioned the possibility of a dynamic WL which can provide additional material for the 3D islands. Although the inclusion of this in the model was found to have little effect on the 3D island density, there were significant effects on the 3D island volume (however, comparison with experiment was not possible). This process is more significant in the high-growth-rate case due to the larger number density of QD's, which

leads to a greater tendency to erode the alloyed WL and hence allow Ga incorporation into the QD's.

V. CONCLUSIONS

We have demonstrated a strong dependence on the InAs deposition rate of the size, composition, and emission wavelength of InAs/GaAs QD's grown by MBE. QD's grown at the lowest rates are larger, have a narrow size distribution, and a higher In content. Low growth rate QD samples encapsulated with GaAs exhibit strong room-temperature emission at $1.3 \mu\text{m}$ with linewidths of $\sim 25 \text{ meV}$. Reduction of the QD growth rate therefore provides a straightforward means to tailor the optical properties. The results demonstrate that the kinetics of QD formation and interplay with the WL play a crucial role in determining the QD properties. In particular, the mechanisms behind QD alloying as a function of temperature and growth rate appear to be very different, and strain-induced detachment of both In and Ga atoms from the WL is likely to be an important process. The qualitative considerations presented here indicate the need for improved atomic-scale understanding of nucleation, growth, and alloying processes in the InAs-GaAs system so that more realistic growth models can be constructed.

ACKNOWLEDGMENTS

This work was supported by the EPSRC, UK. G.R.B. is grateful to the Ramsay Memorial Trust for financial support, funded in part by VG Semicon Ltd. (UK).

*FAX: +44-20-7594-5801; Email: t.jones@ic.ac.uk

¹Y. Arakawa and H. Sakaki, *Appl. Phys. Lett.* **40**, 939 (1982).

²P. Sivers, S. Malik, G. McPherson, D. Childs, C. Roberts, R. Murray, B. A. Joyce, and H. Davock, *Phys. Rev. B* **58**, R10 127 (1998).

³P. B. Joyce, T. J. Krzyzewski, G. R. Bell, B. A. Joyce, and T. S. Jones, *Phys. Rev. B* **58**, R15 981 (1998).

⁴L. Chu, M. Arzberger, G. Böhm, and G. Abstreiter, *J. Appl. Phys.* **85**, 2355 (1999).

⁵G. Park, O. B. Shchekin, D. L. Huffaker, and D. G. Deppe, *Appl. Phys. Lett.* **73**, 3351 (1998).

⁶R. P. Mirin, J. P. Ibbetson, K. Nishi, A. C. Gossard, and J. E. Bowers, *Appl. Phys. Lett.* **67**, 3795 (1995).

⁷H. Ishikawa, H. Shoji, Y. Nakata, K. Mukai, M. Sugawara, M. Egawa, N. Otsuka, Y. Sugiyama, T. Futatsugi, and N. Yokoyama, *J. Vac. Sci. Technol. A* **16**, 794 (1998).

⁸I. Mukhametzhanov, R. Heitz, J. Zeng, P. Chen, and A. Madhukar, *Appl. Phys. Lett.* **73**, 1841 (1998).

⁹K. Nishi, H. Saito, S. Sugou, and J-S. Lee, *Appl. Phys. Lett.* **74**, 1111 (1999).

¹⁰R. Murray, D. Childs, S. Malik, P. Sivers, C. Roberts, J-M. Hartmann, and P. Stavrinou, *Jpn. J. Appl. Phys., Part 1* **38**, 528 (1999).

¹¹J. C. Campbell, D. L. Huffaker, H. Deng, and D. G. Deppe, *Electron. Lett.* **33**, (1997).

¹²J. W. Gray, D. Childs, S. Malik, P. Sivers, C. Roberts, P. N. Stavrinou, M. Whitehead, R. Murray, and G. Parry, *Electron. Lett.* **35**, 242 (1999).

¹³Y. Nakata, K. Mukai, M. Sugawara, K. Ohtsubo, H. Ishikawa,

and N. Yokoyama, *J. Cryst. Growth* **208**, 93 (2000).

¹⁴T. Ngo, P. M. Petroff, H. Sakaki, and J. L. Merz, *Phys. Rev. B* **53**, 9618 (1996).

¹⁵M. Itoh, G. R. Bell, A. R. Avery, T. S. Jones, B. A. Joyce, and D. D. Vvedensky, *Phys. Rev. Lett.* **81**, 633 (1998).

¹⁶D. I. Westwood, Z. Sobiesierski, C. C. Matthai, E. Steimetz, T. Zettler, W. Richter, and D. A. Woolf, *J. Vac. Sci. Technol. B* **16**, 2358 (1998).

¹⁷J. G. Belk, J. L. Sudijono, D. M. Holmes, C. F. McConville, T. S. Jones, and B. A. Joyce, *Surf. Sci.* **365**, 735 (1996).

¹⁸J. G. Belk, C. F. McConville, J. L. Sudijono, T. S. Jones, and B. A. Joyce, *Surf. Sci.* **387**, 213 (1997).

¹⁹M. Sauvage-Simkin, Y. Garreau, R. Pinchaux, M. B. Véron, J. P. Landesman, and J. Nagle, *Phys. Rev. Lett.* **75**, 3485 (1995).

²⁰J. Tersoff, *Phys. Rev. Lett.* **81**, 3183 (1998).

²¹H. T. Dobbs, D. D. Vvedensky, A. Zangwill, J. Johansson, N. Carlsson, and W. Seifert, *Phys. Rev. Lett.* **79**, 897 (1997); H. T. Dobbs, D. D. Vvedensky, and A. Zangwill, in *Surface Diffusion: Atomic and Collective Processes*, edited by M. C. Tringides and M. Scheffler (Plenum, New York, 1997).

²²H. M. Koduvely and A. Zangwill, *Phys. Rev. B* **60**, R2204 (1999).

²³C. Priester and M. Lannoo, *Phys. Rev. Lett.* **75**, 93 (1995).

²⁴Y. Chen and J. Wahsburn, *Phys. Rev. Lett.* **77**, 4046 (1996).

²⁵G. R. Bell, J. G. Belk, C. F. McConville, and T. S. Jones, *Phys. Rev. B* **59**, 2947 (1999).

²⁶Q-K. Xue, Y. Hasegawa, H. Kiyama, and T. Sakurai, *Jpn. J. Appl. Phys., Part 1* **38**, 500 (1999).